TRANSMISSION ELECTRON MICROSCOPY STUDY OF A PRESOLAR SILICATE FROM THE MILLER RANGE 07687 CHONDRITE L. B. Seifert[1], P. Haenecour[1], T. Ramprasad[2], T. J. Zega[1,2]. [1] Lunar and Planetary Laboratory, University of Arizona, 1629 E University Blvd. Tucson, AZ 85721-0092, lseifert@lpl.arizona.edu, [2]Materials Science and Engineering, University of Arizona, Tucson, AZ.

Introduction: Presolar grains are particles of dust that formed in the circumstellar envelopes of evolved stars and in the ejecta of stellar explosions such as novae and supernovae. The detailed analysis of the structure and chemistry of presolar grains offers insight into stellar nucleosynthesis, the thermodynamic conditions under which they formed, as well as their subsequent alteration histories.

Presolar silicate grains in particular are more susceptible to secondary processing and isotopic equilibration than other presolar grain types [1]. For this reason, presolar silicates can be used as tracers of nebular and parent-body processing [1]. We report here the coordinated analyses of a supernova silicate grain from the Miller Range (MIL) 07687 CO3 chondrite. This work is part of a broader effort to study the structure and chemistry of presolar grains within the matrices of altered and unaltered chondrites in order to understand their histories.

Sample and Methods: Isotopically anomalous presolar grains were identified via NanoSIMS raster-ion-imaging of a petrographic thin section of MIL 07687 at Washington University in St. Louis [1]. One grain, MIL '10a2-6 ol' was selected for extraction and detailed chemical and structural analysis using transmission electron microscopy (TEM).

Focused-ion beam scanning-electron microscopy (FIB-SEM) techniques [e.g., 2-3] were used to prepare an electron transparent cross-section of MIL 10a2-6 ol with the Thermo Fisher (formerly FEI) Helios G^3 FIB-SEM located at the Lunar and Planetary Laboratory (LPL). The FIB section was subsequently analyzed using the 200 keV aberration-corrected Hitachi HF5000 scanning TEM (S/TEM) at LPL. The HF5000 is equipped with STEM-based secondary electron (SE), bright-field (BF), and dark-field (DF) imaging detectors, as well as an Oxford Instruments X-Max^N 100 TLE energy dispersive X-ray spectroscopy (EDS) system with dual 100 mm^2 windowless silicon-drift detectors (solid angle of 2 sr).

Results: NanoSIMS analysis of MIL 10a2-6 ol by [1] reveals enrichments in both ^{17}O and ^{18}O relative to solar system values with $^{17}O/^{16}O$ ($\times10^{-4}$) = 4.86 ± 0.15 and $^{18}O/^{16}O$ ($\times10^{-3}$) = 2.56 ± 0.03 (Fig. 1). The isotopic composition of MIL 10a2-6 ol places it in the Group-4 field of presolar grains as defined by [4], which is consistent with origins in the ejecta of a core-collapse supernova.

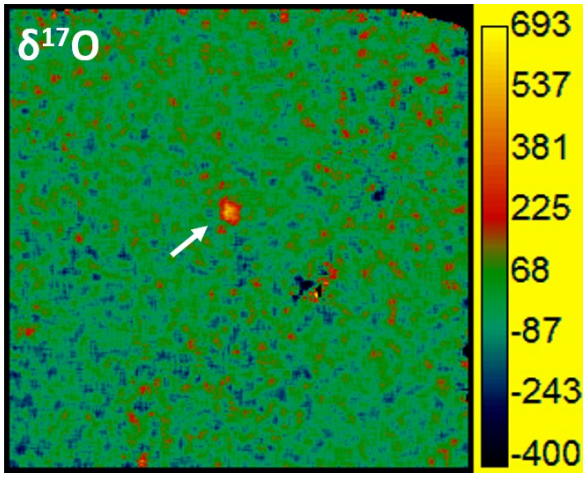

Figure 1: δ^{17}O isotopic map (10µm field of view) of MIL 10a2-6 ol. Legend at right of image in units of per mil (‰).

S/TEM imaging shows MIL 10a2-6 ol is a fine-grained domain below the Pt fiducial marker (dashed outline, Fig. 2a-b). EDS mapping of MIL 10a2-6 ol (Fig. 2c-h) reveals spatial correlations among O, Si, Mg, Ca, and Al. The edges of MIL 10a2-6 ol contain an Fe-rich composition (Fig. 2f). In comparison, the matrix at the top of the FIB section that surrounds MIL 10a2-6 ol is fine-grained, while the remainder of the FIB section (not shown) is porous, and dominated by elongated, fibrous grains that range in size from about 400 nm to 1.4 µm in length. EDS mapping of the whole section shows spatial correlations among O, Si, Fe, Al, Ni and S with localized Ca and Mg. The elongated, fibrous grains contain Fe and O.

Selected-area electron-diffraction (SAED) patterns obtained across MIL 10a2-6 ol show that it is polycrystalline, with d-spacings consistent with a pyroxene. The matrix contained within the FIB section is a mixture of crystalline and amorphous silicates and oxides. An SAED pattern obtained from one of the fibrous grains is consistent with ferrihydrite.

Discussion: The MIL 07687 chondrite matrix contains regions of Fe-poor matrix that is relatively unaltered, and Fe-rich matrix that is relatively altered. Previous work [1] indicates that alteration phases, such as ferrihydrite, dominate the Fe-rich matrix, while the Fe-poor matrix contains isolated fibers of ferrihydrite. The widespread ferrihydrite fibers observed in the FIB section and the Fe-rich composition at the edges of MIL

10a2-6 ol are consistent with descriptions of the Fe-rich (relatively altered) matrix [1]. The presence of ferrihydrite fibers is consistent with previously described aqueous alteration of a fine grained matrix under highly oxidizing conditions or terrestrial weathering [1].

Comparison of the structure and chemistry of presolar grains with thermodynamic model predictions can help constrain their origins. Equilibrium and kinetic models of dust condensation specific to supernovae are limited, but some data are available in the literature [4-5]. Compared to equilibrium predictions, Ca-bearing pyroxene is predicted to condense between 1082 and 1560 K [5]. Alternatively, kinetic models do not explicitly discuss Ca-bearing pyroxenes, but do note that Mg-silicates are expected to condense between 1400 and 1500 K [6] and also around 1100 K [7].

Polycrystalline and amorphous presolar grains were previously reported in the literature and are thought to suggest either nonequilibrium or multistep condensation processes [8-11]. We do not observe amorphous grains in the MIL 10a2-6 ol domain or in the material that immediately surrounds MIL 10a2-6 ol which argues against a nonequilibrium formation process. We hypothesize that as temperatures cooled in the ejecta of the host supernova, nanocrystalline pyroxene grains condensed and mechanically accreted together to form the assemblage we observe. Further, the TEM data suggest that even though MIL 10a2-6 ol was extracted from an Fe-rich matrix region, the grain was preserved in fine-grained material that escaped significant parent-body processing.

Acknowledgments: We thank Adrian Brearley for loaning us the MIL 07687 thin section. The research completed here was supported by NASA grants NNX15AJ22G and 80NSSC19K0509. We also acknowledge NASA grants NNX12AL47G, NNX15AJ22G, 80NSSC19K0509, and NSF grant 1531243 for funding instrumentation in the Kuiper Materials Imaging and Characterization Facility at LPL.

References: [1] Haenecour P. et al. (2020) *Meteoritics & Planet. Sci., 55*, 1228-1256. [2] Zega T. J. et al. (2007) *Meteoritics & Planet. Sci., 42*, 1373-1386. [3] Seifert L. et al. (2022) *Meteoritics & Planet. Sci.,* in revision. [4] Nittler L. et al. (1997) *ApJ 483*, 475-495. [5] Fedkin A. V. et al. (2010) *GCA* 74, 3642-3658. [6] Nozawa T. et al. (2003) *ApJ*, 598, 785-803. [7] Todini P. and Ferrara A. (2001) *MNRAS* 325, 726-736. [8] Stroud, R. M. et al. (2009) *LPC*, 40, 1063. [9] Vollmer, C. et al. (2009) *ApJ*, 700, 774-782. [10] Nguyen, A. N. et al. (2010) *ApJ,* 719, 166-189. [11] Zega, T. J., et al. (2020) *Meteoritics & Planet. Sci., 55*, 1207-1227.

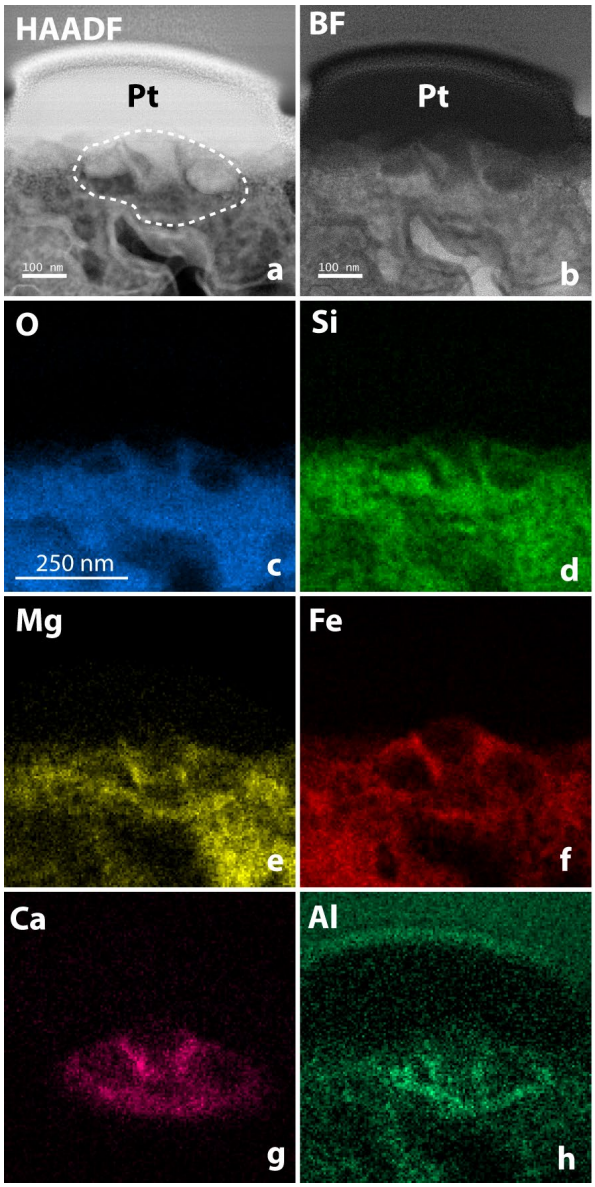

Figure 2: S/TEM data on MIL 10a2-6 o1. (a-b) HAADF and BF-STEM images of MIL 10a2-6 o1 below Pt fiducial marker. (c-h) False color EDS maps for O, Si, Mg, Fe, Ca, and Al, respectively.